JOURNAL OF MATERIALS SCIENCE 12 (1977) 1109–1114

Retardation of the precipitation reaction by d.c. stress in an Al-12.5 wt % Zn alloy

YUKIO ONODERA, JUN-ICHI MARUYAMA*, KEN-ICHI HIRANO
Department of Materials Science, Faculty of Engineering, Tohoku University, Sendai 980, Japan

The effect of direct electric current stress on the precipitation reaction in an Al–12.5 wt % Zn alloy was investigated by the resistometric method. It was found that the d.c. stress retarded the reaction rate as in the case of an Al–4 wt % Cu alloy. The dependence of the retarding effect on the annealing time and on the quenching temperature was examined on the basis of a model of current-assisted vacancy annihilation. The annealing temperatures after quenching were 30 and 40° C, and the quenching temperatures were varied from 300 to 500° C.

1. Introduction

In a previous work [1] we investigated the stress effect of direct electric current on the precipitation reaction in a quenched Al–4.15 wt % Cu alloy and found that the d.c. stress retarded the precipitation reaction. We suggested that this effect was due to the sweeping out of quenched-in excess vacancies assisted by direct electric current into sinks such as grain boundaries and/or dislocations. A theoretical expression for this model was also proposed.

The purpose of the present work is to confirm the presence of the retarding effect more definitely than in the case of an Al–4.15 wt % Cu alloy by using an Al–Zn alloy, since we already knew from our preliminary experiments [2–4] that in an Al–8.4 wt % Zn alloy the d.c. stress retarded the precipitation of the GP zones under proper experimental conditions. Moreover, since the Al–Zn system has an extended solubility limit of zinc in aluminium for a wide range of temperatures, it is expected that the concentration of quenched-in excess vacancies can be changed more widely than that in the Al–Cu system.

2. Experimental method

Ingot bars of an Al–12.5 wt % Zn were prepared from an Al–18.2 wt % Zn mother-alloy by induction heating. After the bar was annealed for 140 h in air, a portion of the ingot bar was cold-swaged and then drawn into wires of 0.37 mm diameter. The main impurities in the specimen wire were 0.001 wt % Fe and 0.001 wt % Si. The method of holding the specimen and of measuring the resistivity were the same as described in [1].

A freshly prepared specimen was annealed for about 2 h at a higher temperature ($\simeq 500°$ C) than a quenching temperature in order to reduce some of the structural change brought into the specimen during a sequence of such repeated heat-treatments as homogenization, quenching and annealing. The specimen was kept for less than 30 min at a homogenization temperature and then quenched in iced water. After quenching the power annealing was carried out in a voluminous water bath ($\simeq$ 50 litre). The water in the bath was stirred with four mechanical stirrers and it was circulated in the immediate vicinity of the specimen with a pressure pump as well, in order to reduce the temperature increase in the specimen caused by the Joule heating. The pressure pump was not used in the experiment of d.c. stress effect on the isothermal annealing curve, which will be described in the next section.

3. Experimental results

3.1. Effect of d.c. stress on isothermal annealing curves

Fig. 1 shows one example of an isothermal an-

* Present Address: Central Engineering Laboratory, Nissan Motor Co Ltd, Natsushima-cho, Yokosuka 237, Japan.

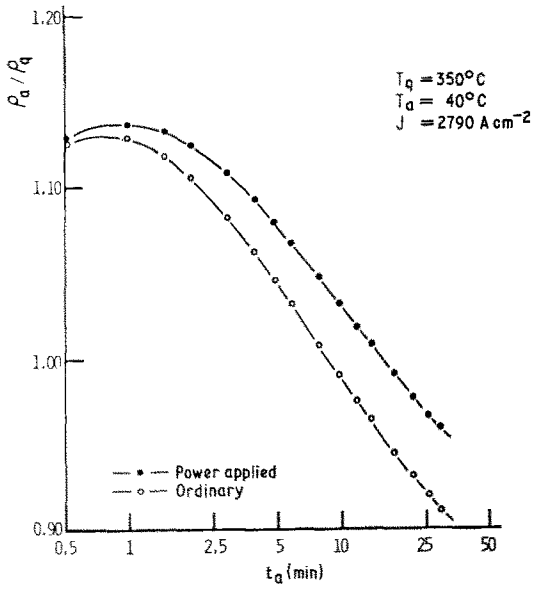

Figure 1 Isothermal annealing curves at 40° C after quenching from 350 to 0° C in an Al–12.5 wt % Zn alloy, with (—•—) and without (—○—) d.c. stress. The resistivity ratio ρ_a/ρ_q is plotted as a function of the annealing time, where ρ_a and ρ_q are the resistivities after annealing and quenching, respectively.

nealing curve at 40° C for the specimen quenched from 350° C with and without d.c. stress during annealing. The resistivity ratio ρ_a/ρ_q is plotted against the annealing time, where the subscripts a and q denote annealing and quenching respectively. The stress current density during this power annealing was 2790 A cm^{-2}. In this case, a retarding effect on the precipitation reaction similar to that observed in an Al–4.15 wt % Cu alloy [1] was more clearly noticeable. Similar results to those in Fig. 1 were also obtained at various stress current densities from 470 to 2330 A cm^{-2} and these are presented in Fig. 2, where the fractional change in the specimen resistivity $(\rho^J - \rho^O)/\rho^O$ caused by power annealing is plotted versus the annealing time, and where ρ^J and ρ^O denote the specimen resistivities measured at liquid nitrogen temperature after being subjected to power and ordinary annealing, respectively. In practice, the values of $(\rho^J - \rho^O)/\rho^O$ have been calculated from the following relation:

$$(R_a^J/R_q^J - R_a^O/R_q^O)/(R_a^O/R_q^O)$$
$$= \{(\rho_a^J/\rho_q^J)(\rho_q^O/\rho_a^O) - 1\}$$
$$= (\rho_a^J - \rho_a^O)/\rho^O \quad (\text{since } \rho_q^J = \rho_q^O)$$

where R is the specimen resistance, the subscripts a and q represent annealing and quenching respectively, and the superscripts J and O distinguish the specimens: specimen J was used for power annealing and specimen O for ordinary annealing. In general, the retarding effect becomes noticeable with increasing the stress current density, as seen in Fig. 2, and it tends to saturate as the annealing time is increased. Furthermore, when the stress current density is less than 1400 A cm^{-2}, the magnitude of the retarding effect begins to decrease slightly after passing a maximum. At present it is not known whether this is due to some

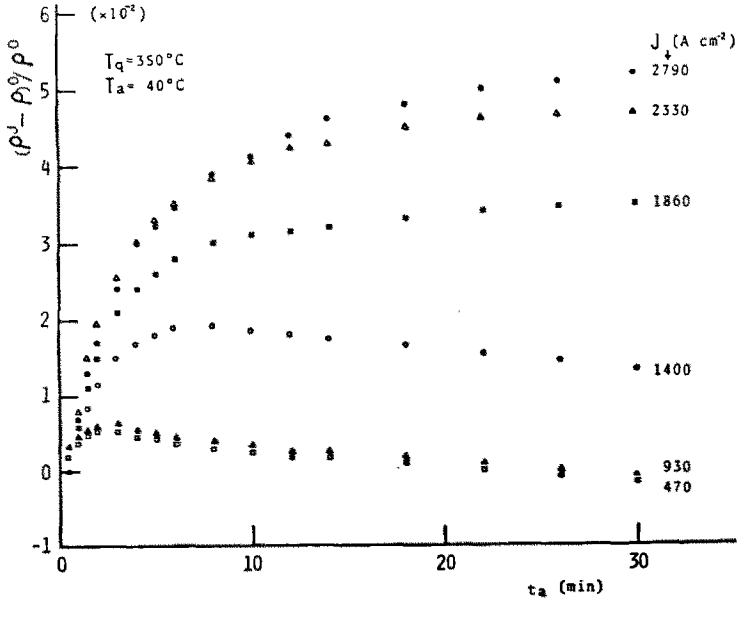

Figure 2 Effect of d.c. stress on the isothermal annealing curve under various current densities. Fractional change in the resistivity $(\rho^J - \rho^O)/\rho^O$, is plotted as a function of the annealing time, where ρ^J is the resistivity of a powered specimen and ρ^O is the resistivity of a reference specimen.

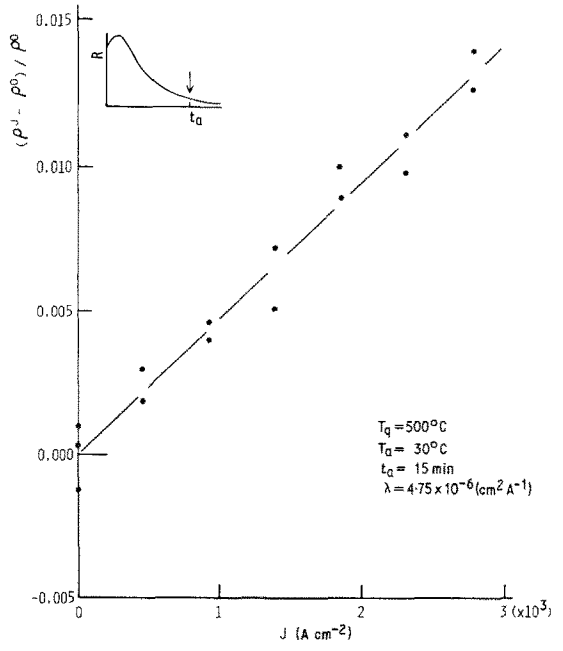

Figure 3 Current dependence of the fractional change in the specimen resistivity caused by power annealing. In the same figure, an isotherm is schematically given in order to show the corresponding stage to where the measurement was done.

Joule heating effect or not. We shall comment on this point in a later section.

3.2. Dependence of d.c. stress effect on quenching temperatures

In order to obtain more reliable information about the dependence of the retarding effect on quenching temperatures, we employed a somewhat different procedure from the one in the previous section. The retarding effect was measured as a function of the stress current density at a given quenching temperature T_q, annealing temperature T_a and annealing time t_a. A typical result for $T_q = 500^\circ$ C, $T_a = 30^\circ$ C and $t_a = 15$ min is shown in Fig. 3. An isothermal annealing curve is also schematically presented in this figure to show the corresponding stage to t_a. We obtained a linear relation between the values of $(\rho^J - \rho^O)/\rho^O$ and the stress current J, as suggested in [1], and we defined the slope of this straight line to be the "retarding coefficient", $\lambda\{\equiv(\rho^J - \rho^O)/(\rho^O J)\}$. The retarding coefficients thus determined under various experimental conditions are shown in Fig. 4, where, for convenience, λ is plotted versus the annealing time. At a given annealing temperature of $T_a = 30^\circ$ C, the retarding

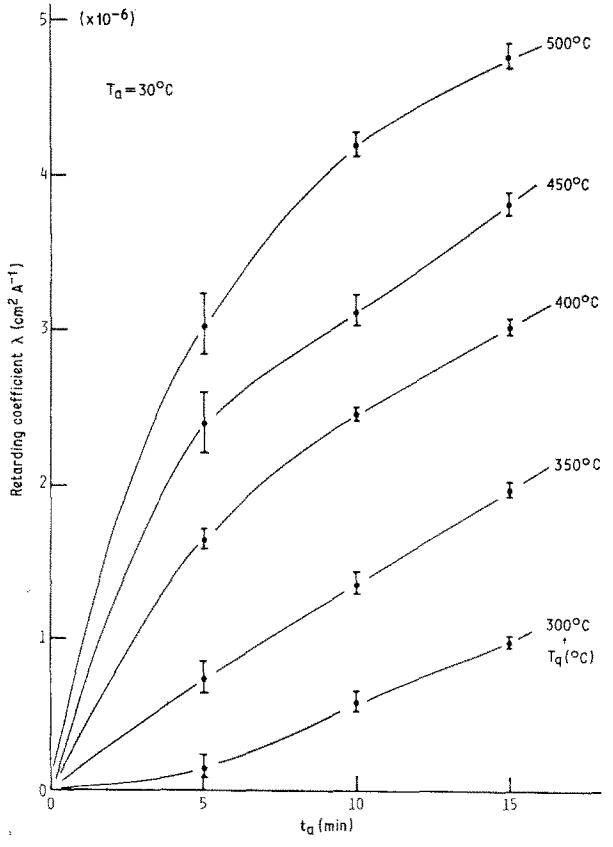

Figure 4 Dependence of the retarding coefficient on the annealing time after quenching from various temperatures. The values of the retarding coefficient was obtained from the slopes of such curves as in Fig. 3 at a given quenching temperature and annealing time.

coefficient increases as we increase the quenching temperature and the annealing time. It is possibly meaningless to compare the present results with those in Fig. 2 because the results in Fig. 2 may be affected by the Joule heating effect more seriously.

4. Discussion

4.1. A kinetic equation describing d.c. stress effect on the precipitation reaction

Since Equation 10 in [1], which describes the retarding effect on the basis of a model of current-assisted vacancy annihilation, involves several ambiguous points, let us present a more explicit explanation of that formulation. Equation 10 in [1] is

$$\frac{\rho^{J}-\rho^{O}}{\rho^{O}}=\frac{KN_{v}(O)D_{v}|eZ^{*}|\rho}{\gamma dkT\rho^{O}}\left(\frac{1}{\gamma}-\frac{e^{-\gamma t}}{\gamma}-te^{-\gamma t}\right)J. \tag{1}$$

Strictly speaking, the factor ρ/ρ^{O} appearing on the right-hand side in this equation depends on the annealing time $t_a(\equiv t)$, so that it should be expressed as

$$\frac{\rho}{\rho^{O}}\equiv\frac{\rho^{J}(T_a,t_a)}{\rho^{O}(t_a)}=\frac{\rho^{J}(t_a)}{\rho^{O}(t_a)}+\frac{\Delta}{\rho^{O}(t_a)}, \tag{2}$$

where $\rho\equiv\rho^{J}(T_a, t_a)$ is the specimen resistivity during power annealing at an annealing temperature of T_a and at an annealing time of t_a after quenching. The quantities $\rho^{J}(t_a)$ and $\rho^{O}(t_a)$, in which no temperature is specified, are the resistivities measured at liquid nitrogen temperature after quench-annealing at T_a for t_a. Δ is the difference of the resistivity between an annealing temperature T_a and the liquid nitrogen temperature ignoring the time dependence of Δ. If we abbreviate T_a by T and t_a by t, then Equation 1 can be rewritten as

$$\frac{\rho^{J}(t)-\rho^{O}(t)}{\rho^{O}(t)}=\frac{KN_{v}(O)D_{v}|eZ^{*}|}{\gamma^{2}dkT}\left[\frac{\rho^{J}(t)}{\rho^{O}(t)}+\frac{\Delta}{\rho^{O}(t)}\right]\times(1-e^{-\gamma t}-\gamma te^{-\gamma t})J. \tag{3}$$

If we solve Equation 3 for $\rho^{J}(t)/\rho^{O}(t)$ approximately under the condition

$$\frac{KN_{v}(O)D_{v}|eZ^{*}|\rho(1-e^{-\gamma t}-\gamma te^{-\gamma t})J}{\gamma^{2}dkT}\ll 1, \tag{4}$$

and leave only the linear term with respect to J, we obtain

$$\frac{\rho^{J}(t)-\rho^{O}(t)}{\rho^{O}(t)}\approx\frac{KN_{v}(O)D_{v}|eZ^{*}|}{\gamma^{2}dkT}\left[1+\frac{\Delta}{\rho^{O}(t)}\right]\times(1-e^{-\gamma t}-\gamma te^{-\gamma t})J, \tag{5}$$

a somewhat modified form of Equation 1.

As was done in [1], Equation 5 was derived assuming that both K and γ^{J}, appearing in Equations 4, 4a and 6 in [1], are independent of annealing time. The time dependence of γ^{J} is only apparent because we can keep it constant during power annealing by using an electric field E, instead of a current density J, as an external control parameter. This situation can readily be understood from the following expression: $\gamma^{J}=\gamma[1+D_{v}|eZ^{*}|\rho^{J}(T, t)J/\gamma dkT]$, where $\rho^{J}(T, t)J$ can be replaced with E. Of course, here we have assumed that the time dependence of γ^{J} is introduced only through $\rho^{J}(T, t)$. On the other hand, although there is no physical reason to assume K is constant with the resulting first order rate equation $-d\rho/dt=KN_{v}^{O}$ in [1], we use this simple kinetic equation as a

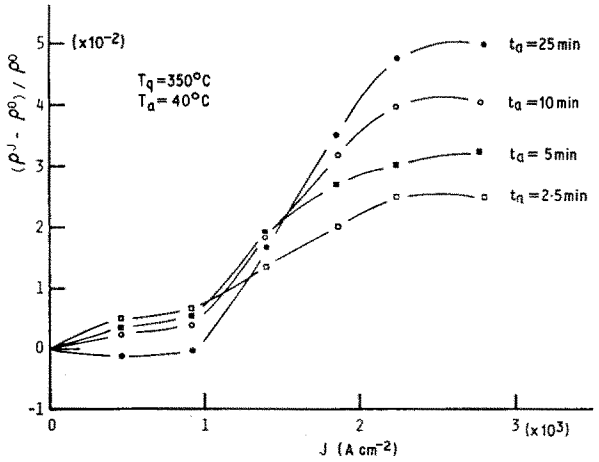

Figure 5 Current dependence of the fractional change in the specimen resistivity caused by power annealing, obtained from replotting the results of Fig. 2.

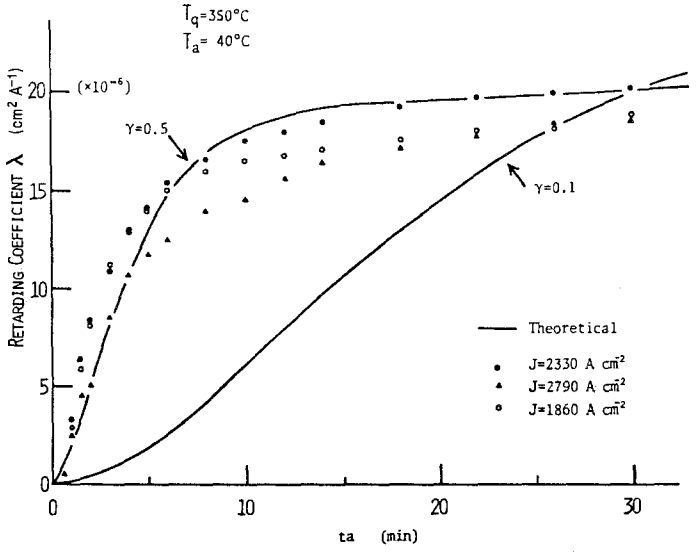

Figure 6 Comparison of the time dependence of the retarding coefficient between experimental and theoretical values. Two examples of the theoretical curve are shown, where γ is assumed to be 0.5 and 0.1.

starting point since we can find no other reliable kinetic equation which describes the precipitation reaction investigated here, nor any exact relation connecting a physical quantity such as the electrical resistivity with a microscopic quantity such as the excess vacancy concentration of a specimen.

4.2. Time dependence of d.c. stress effect

In the experiments shown in Figs. 1 and 2, there was no partial circulation around the specimens, as we already stated in Section 2, so that large contribution of the Joule heating effect to the retarding effect on the strong side of the stress current would be expected from the experimental result of Section. 3.2. In order to confirm this, we replotted the data of Fig. 2 versus the stress current density J as shown in Fig. 5. The result shows that the curves follow case 2 in [1] as expected, except on the weak side of the stress current; however, the presence of a threshold current density ($\simeq 1000$ A cm^{-2}) cannot be understood. Furthermore, at present, we still do not have any knowledge about the time dependence of the Joule heating effect on the retarding effect. Taking all this into account, we have excluded the data of stress current densities less than 1400 A cm^{-2}, which show a tendency to decrease after passing a maximum, from the following discussion.

In Fig. 6, we present the theoretical curves of the retarding coefficient according to Equation 5, as well as the experimental values obtained from Fig. 2. The theoretical curves given in Fig. 6 are drawn semi-empirically using Equation 5 which has been normalized using an experimental value of $\lambda = 2 \times 10^{-5}$ cm^2 A^{-1} at 30 min and assuming γ to be 0.5 or 0.1. The factor $[1 + \Delta/\rho^{O}(t)]$ was estimated from another independent experiment, where we obtained $\Delta = 2.33\,\mu\Omega$ cm. The value of 0.5 for γ was chosen in a fairly arbitrary way to fit the experimental values as smoothly as possible. 0.1 was the maximum experimental value for γ from an isothermal annealing curve at 30° C after quenching from 350° C, assuming the first order reaction for the kinetic equation applies over the decreasing stage of the specimen resistivity in such curves as in Fig. 1. The values of γ obtained in this way are in the range from 0.1 to 0.05 since the annealing curve did not necessarily follow a first order reaction over the entire annealing-time range investigated. The value of 0.5 for γ is tentative since it is larger than the experimental values obtained above. Thus, we can only say that the experimental values of the retarding coefficients are in qualitative agreement with the theoretical curves in that they increase steeply with increasing the annealing time and then approach saturated values.

4.3. Dependence of d.c. stress effect on quenching temperatures

According to Equation 5, the retarding coefficient should be proportional to the initial concentration $N_v(O)$ of quenched-in excess vacancies at a given annealing temperature and time: $\lambda \propto N_v(O)$. Furthermore, the concentration of quenched-in excess vacancies can be expressed as $N_v(O) \propto \exp(-E_f/kT_q)$, where E_f is the vacancy formation

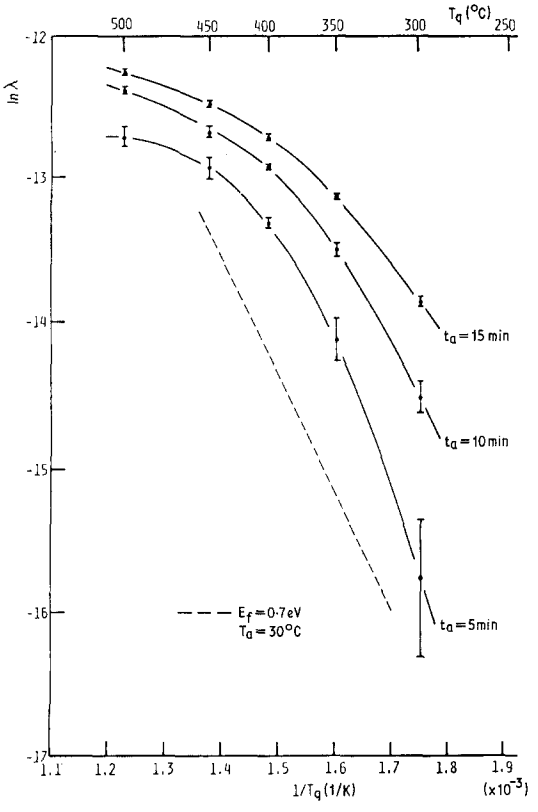

Figure 7 Dependence of ln(λ) on the reciprocal quenching temperature. The slope of the line which is assumed to be $E_f = 0.7$ eV is also given by a broken line as a reference.

energy, k is Boltzmann's constant and T_q is the quenching temperature. Hence, the slope of λ versus $1/T_q$ curve will give E_f. However, as seen in Fig. 7, the plots obtained experimentally do not necessarily follow a single straight line and the slopes tend to decrease with increasing the quenching temperature. This may be due to the fact that the fraction of quenched-in excess vacancies lost during quenching becomes large with increasing the quenching temperature. The activation energies obtained from these slopes are in the range from 0.40 to 0.98 eV. If we take into consideration the simplicity and the various approximations introduced into the derivation of Equation 5, these activation energies agree fairly well with the available vacancy formation energy of an aluminium alloy (around 0.7 eV).

References

1. Y. ONODERA and K. HIRANO, *J. Mater. Sci.* **11** (1976) 809.
2. S. TANAKA, Y. ONODERA and K. HIRANO, presented in part at the spring meeting of the Japan Institute of Metals, April 1973, abstract p. 29 (in Japanese).
3. J. MARUYAMA, Y. ONODERA and K. HIRANO, presented in part at the autumn meeting of the Japan Institute of Metals, November 1974, abstract p. 232 (in Japanese).
4. J. MARUYAMA, Y. ONODERA and K. HIRANO, presented in part at the autumn meeting of the Japan Institute of Metals, October 1975, abstract p. 237 (in Japanese).

Received 11 October and accepted 28 October 1976.